International Journal of Computational Methods and Experimental Measurements
https://www.acadlore.com/journals/IJCMEM

Experimental and Numerical Evaluation on the Flexural Behavior of Concrete Beams with Embedded Functional Plates

Majid Muttashar*, Douaa Najah

Department of Civil Engineering, College of Engineering, University of Thi-Qar, 64001 Nasiriyah, Iraq

* Correspondence: Majid Muttashar (majid-alzaidi@utq.edu.iq)

Received: 10-25-2025 **Revised:** 12-09-2025 **Accepted:** 12-24-2025

Citation: M. Muttashar and D. Najah, "Experimental and numerical evaluation on the flexural behavior of concrete beams with embedded functional plates," *Int. J. Comput. Methods Exp. Meas.*, vol. 13, no. 4, pp. 815–830, 2025. https://doi.org/10.56578/ijcmem130406.

Abstract: Functional plate is one of the most typical materials used for strengthening of reinforced concrete (RC) structures. This article focuses on using functional plates internally to improve the flexural response of RC beams. For this purpose, experimental and numerical investigations on the flexural behavior and ductility of steel-plated RC beams were conducted. Nine RC beams were cast and cured for 28 days. The steel plates were located at the tension side of the RC beams to investigate their effect on the flexural performance of the tested beams. To achieve the research objective, three configurations of the shape of steel plates were proposed, flat, curved, and rounded. The results demonstrate that using embedded steel plates is effective and significantly enhanced the flexural performance of concrete beams. The strengthening delayed the first cracking appearance and increasing of ultimate load up to 45% compared to the reference beam. Further, there was an improvement in ductility and stiffness behaviours by 202% and 46%, respectively, particularly for beams with constrained flat steel plates, which exhibited the highest performance gain. The experimental and finite element (FE) results showed a good agreement in terms of cracking behavior and with approximately 6% maximum ultimate load difference.

Keywords: Reinforced concrete beams; Flexure; Embedded steel plate; Ductility; Stiffness; Finite element; ABAQUS

1 Introduction

Worldwide, many buildings are increasingly susceptible to damage due to earthquakes, ageing, natural disasters, and corrosion of rebars, etc. Several strengthening techniques were used to mitigate these challenges, including section enlargement [1, 2], externally bonded steel plating [3–5], wrapping with fiber reinforced polymer (FRP) composites [6, 7], and employing external post-tensioning. Each strengthening technique possesses some limitations, such as difficulty in implementation, excessive costs, reduction of headroom, aesthetic degradation, demanding special surface preparation, increased self-weight, and potential debonding failure in some techniques [8]. Moreover, a limited number of research studies examined the concept of steel plate reinforcement [9–12]. In such a technique, steel plates are utilized externally as a strengthening way for the deterioration of structures after natural disasters or extended service and other reasons. Metawei et al. [13] conducted an experimental study on the flexural performance, ductility, and stiffness of a reinforced concrete (RC) beam containing chequer steel plates as additional reinforcement on the tension side of the section, considering the surface roughness of the two faces of the plates. The results showed a 27% improvement in the ductility of beams incorporating rough steel plates compared with beams containing smooth plates. This finding revealed that chequer plates represent an appropriate alternative for regular reinforcement. Sarhan et al. [14] performed an experimental investigation on the strength and the ductility of steel-plated RC beams. They concluded that, in comparison to the reference beam, the ductility increased by an average of three times; further, the study indicated that connecting the plates with bolts was a more reliable method of improving the ductility than employing angles. Ibrahim et al. [15] presented an investigation of the flexural performance of self-compacting reinforced concrete beams (SCC) with the incorporation of internal steel plates. The research parameters included plate thickness and spacing between plates. The results highlighted that the yielding load of beams containing steel plates was lower than the yielding load of the reference beam by 5.21%. In contrast, the deflection increased by 13.72% at the yield load, while the ultimate load was 6.77% lower than the reference beam. In terms of the

ductility, there was a drop of 20.08%. They explained that this behavior might result from the redistribution of stress that is caused by the hardening of stress, which occurs in the main reinforcement, which lowers the beam's neutral axis, increases the depth of the compression zone, and influences the cracked moment of inertia. Ammash [16] conducted an experimental and theoretical study to assess the effect of substituting steel stirrups with steel plates as shear reinforcement. The results concluded that incorporating steel plate as shear reinforcement could enhance the shear capacity. The increase of the plates' width and reduction of the interspacing between the plates resulted in control on crack width and a decrease in the number of cracks, which enhances the concrete confinement. Ibrahim et al. [17] experimentally investigated the validity of using shear steel plates for the behavior of wide RC beams. They determined that the shear steel plates were an excellent alternative for stirrups, demonstrating agreeable outcomes for yield and final loads. In addition, the ductility improved by 55%, whereas the strain of the interior and exterior legs decreased by 46% and 17%, respectively. Furthermore, the weight of the wide beam reduced by 2.7%. In contrast, increasing the spacing between the shear steel plates reduces the yield load and increases the deflection at yield. Liu et al. [18] experimentally and theoretically explores the mechanical properties of RC beams incorporating steel plates of various shapes. Flat and corrugated steel plates with different thickness, wave height and strength embedded at the tension side of the beam to investigate their effect on the flexural performance of the reinforced beam. The results indicated that the corrugated steel plate showed a significant reinforcing effect by enhancing the bearing loads and improving the deformation's resistance. Ding et al. [19] conducted a full-scale test on concrete tunnel segment joint reinforced with steel corrugated plate. Their results demonstrate that the major failure was crushing of concrete in the compression zone. Moreover, there was an increase of 73.7% and 119.3% in the moment capacity and the ultimate load of the reinforced segment compared with the unreinforced joint, respectively. The results reflect the significant effect of the corrugated steel plate on the flexural behavior of the tested samples due to the higher stiffness of the plate. Yu et al. [20] conducted a bending test to investigate the load-carrying performance of five concrete beams reinforced with flat and corrugated steel plates. The results show that the thickness of the plate has significant effect on the flexural behavior regardless of the plate type. Moreover, beams reinforced with corrugated steel plate exhibit better enhancement compared with the beams reinforced with flat steel plate. The study proposed a theoretical formula to determine the moment of inertia of the combined section. Steel plates in (flat and corrugated) shapes were used to strengthen the original building by erecting them inside the existing structure and filling the gaps with concrete. This technique creates a cohesive bond that can be stressed together [21, 22].

Despite the progress made, the literature demonstrates that most of the existing research focuses on the flexural behavior of concrete beams externally strengthening with steel plates. Moreover, a limited understanding of the effect of internal steel plates on the flexural performance of the concrete beams, especially the plate configuration, orientation and the holes in the plate. Thus, this study conducts an experimental and numerical evaluation on the effect of using embedded functional steel plate on flexural behavior, crack pattern, mode of failure, ductility and stiffness of concrete beams. The steel plates are used as additional tensile reinforcement. This study made special attention to the role of the steel-concrete bond to explore the possibility of reducing the amount of primary reinforcement by including a limited area of steel plates in the tension side of the cross-section of the beams which has not been sufficiently addressed by previous studies.

2 Methodology

2.1 Material Properties

For a target cubic compressive strength of 25 MPa, the concrete mixture was designed with mix proportions of 1:2.22:3.23 (cement: sand: coarse aggregate) and a water-to-cement ratio of 0.37. The mix design was prepared using coarse and fine aggregates in a saturated surface dry (SSD) condition, with specific gravities of 2.74 and 2.65, respectively. The sieve analysis results of the aggregates are presented in Figure 1. Table 1 presents the mixed proportions. Also, for a standard concrete, a slump test was established to verify the workability of the mixture and to make sure it matches the specifications of ACI: 211.1-91 [23], which refers to the value of slump for beams must range (20–100) mm. Concerning the steel reinforcement, steel reinforcement bars were provided and tested according to ASTM A615/A615M-20 [24], see Table 2. Steel plates were locally supplied with 4mm thickness, then tested according to ASTM A370-05 [25], see Table 3.

Table 1. Concrete mixture's proportions

Materials	Mixture Proportions
Cement (kg/m^3)	325
Fine aggregate (kg/m^3)	720
Coarse aggregate (kg/m^3)	1050
Water (L/m^3)	120

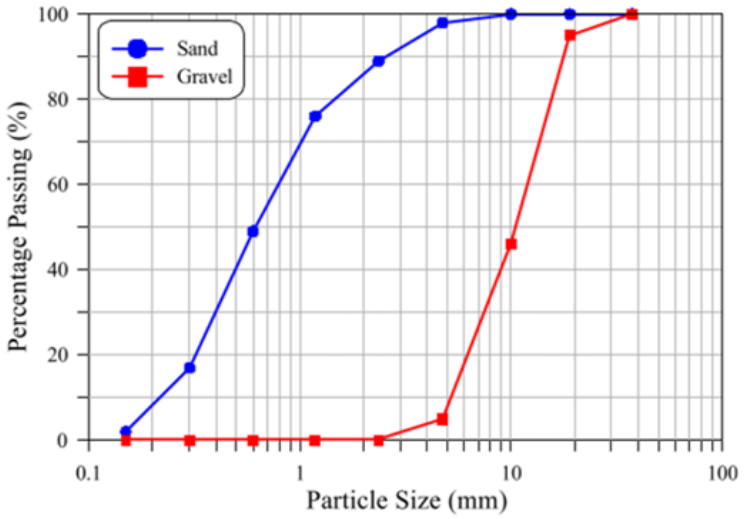

Figure 1. Sieve analysis of the aggregates used in the current study

Table 2. Characteristics of steel reinforcement bars

Type of Steel	Diameter (mm)	Average Yield Stress (N/mm^2)	Min. Limit of Yield Stress (N/mm^2)	Average Ultimate Stress (N/mm^2)	Min. Limit of Ultimate Stress (N/mm^2)	Average Elongation (%)	Min Limit for Elongation (%)
Grade 60	10	590	420	800	620	12.33	9

Table 3. Characteristics of steel plates

Thickness (mm)	Average of Yield Tensile Strength (MPa)	Average of Ultimate Tensile Strength (MPa)	Elongation at Ultimate Stress (%)
4	260	385	24

2.2 Specimens Preparation and Strengthening Procedure

Nine RC beams with a cross sectional-area of (150 × 200) mm and a total length of (1200) mm were cast and cured for 28 days. Figure 2. Showed the details of the reference beam. Referring to steel plates, three configurations were utilized, flat, curved, and rounded. Based on the diameter of the rounded plate, the dimensions of all configurations of the used plates were determined, as shown in Figure 3. In this study, the plates were located at the tension side of the RC beams to investigate their contribution to the flexural performance of the tested beams. To achieve the objective of this research, different configurations were proposed, as shown in Figure 4. Sample labeling was adopted to identify the parameters where the letter refers to the plate shape. No. 4 represents plate thickness, and the second number refers to the side plate configuration, 0 means no plate, 1 means vertical plate and 2 means inclined plate.

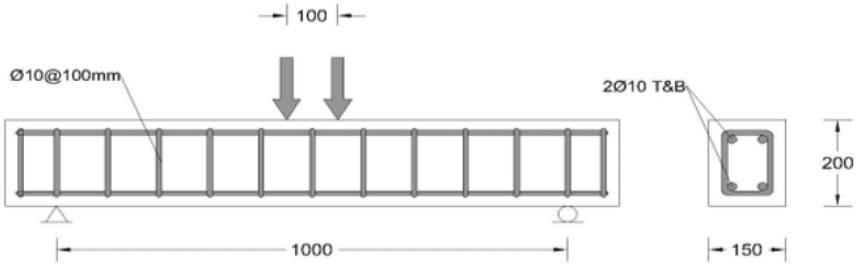

Figure 2. Reference beam details

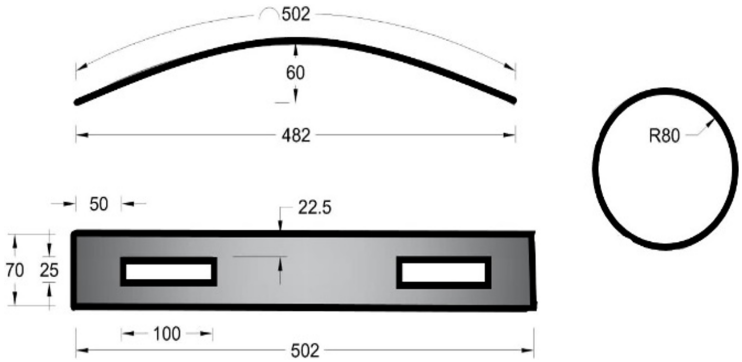

Figure 3. Steel plates' details (dimensions in millimeters)

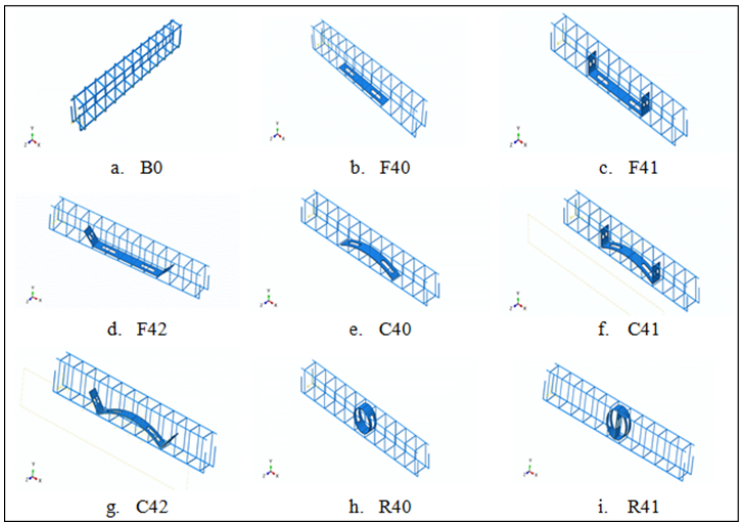

Figure 4. Details of specimens

2.3 Experimental Set-Up

Over the test, four-point loads configuration using a hydraulic jack with a capacity of 150 kN were conducted to load the beams until failure. The distance between points of loading was 100 mm. The load was employed at a constant rate of 1.2 kN/s, also measured by a load cell positioned over the spreader beam, as shown in Figure 5. A positioned LVDT tool was used to measure the mid-span deflection, which connected to the data logger. The specimens were simply supported, with pinned support at one end and roller support at the other, allowing free rotation and longitudinal movement.

Figure 5. Laboratory loading setup

3 Results and Discussion

3.1 Crack Patterns and Failure Modes

The cracks in the flexural members start at the extreme tension fiber of concrete when the tensile stresses exceed the modulus of rupture. For the reference beam (B0), the first crack appears at load of 9 kN precisely opposite to the applied load. Then, a few cracks occur and propagate to the upper side of the beam. After yielding steel, the concrete at the compression zone crushed which results in a total failure of the beam. This type of failure occurred when the beam was under reinforced and called flexural tension failure. In general, specimens reinforced with flat steel plates were recorded the same behaviour, specifically in crack patterns. Comparatively, most cracks were classified as flexural cracks in all specimens except beam F42, in which the cracks were distributed to the shear zone (i.e., near supports) and recorded the highest number of cracks. Concerning specimens reinforced with curved steel plates, the number of cracks is higher than the other two groups (i.e., specimens reinforced with flat and rounded steel plates, respectively). This effect occurred due to the shape of functional plate; with the increase of loading, the sides of plates pull-down and caused extra deformation in concrete and for this reason lateral functional plates added to constrain the sides of curved steel plates in order to improve the bond effect between plates and concrete. Comparatively, the dominant pattern of cracks in specimens reinforced with rounded steel plates was flexure and noticed that the failure's mode was flexure for all beams. Also, the yielding of reinforcement has been the first indication of failure followed by a crush in the R40 specimen. Briefly, using steel plates improves the flexural performance of concrete beams by postponing the formation of pre-cracking by a higher ratio of 155.56% compared with the reference beam. Figure 6 shows the crack patterns of all tested samples.

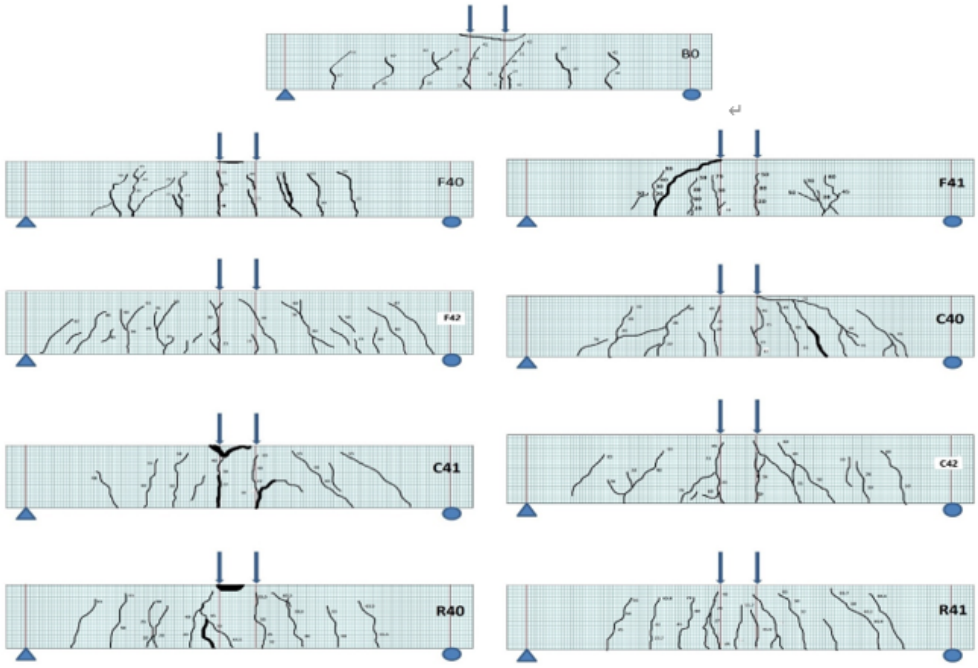

Figure 6. Crack patterns of all tested specimens

3.2 Load-Deflection Behavior

Deflection corresponding to each increment of load at mid-span has been reviewed in Figure 7. As shown in the stated figure, each curve has a comparatively same character if compared to the reference beam. All curves consist of an initial linear elastic portion in which load and deflection were closely proportional. With the increase of load, deflection increases at a slow rate until the propagation of the first crack, then load and deflection are no longer proportional until curves reach the peak value at the final load. Eventually, the load capacity of the beams is reached. All curves exhibit a ductile branch after the ultimate load is reached (i.e., the load dropped slightly until failure). For the reference beam, the first stage in the load-deflection curve started with the beginning of loading. So, this stage continued until the appearance of the first crack at 9kN and corresponding deflection was 0.51mm, respectively. After these values, the deflection began to increase rapidly, and the nonlinear stage started. The peak load and its related deflection were 61.89 kN and 10.18 mm, respectively. After the dropping of load, the test no longer continued, and the concrete crushing under unit loads to announce the end of the test at deflection of 10.37mm. Table 4 shows the experimental results. The above-stated figure and table concluded that the employment of functional plates can

improve the yield load and load-carrying ability by an average increase up to 44.5% and 33%, respectively, compared to the reference beam. Practically, the samples that strengthened with flat steel plate show higher enhancement in the yield and peak loads by 41.91% and 34.91%, respectively, rivaling the reference beam. The reason for that was the position of the functional plate, which is located in the maximum positive moment zone.

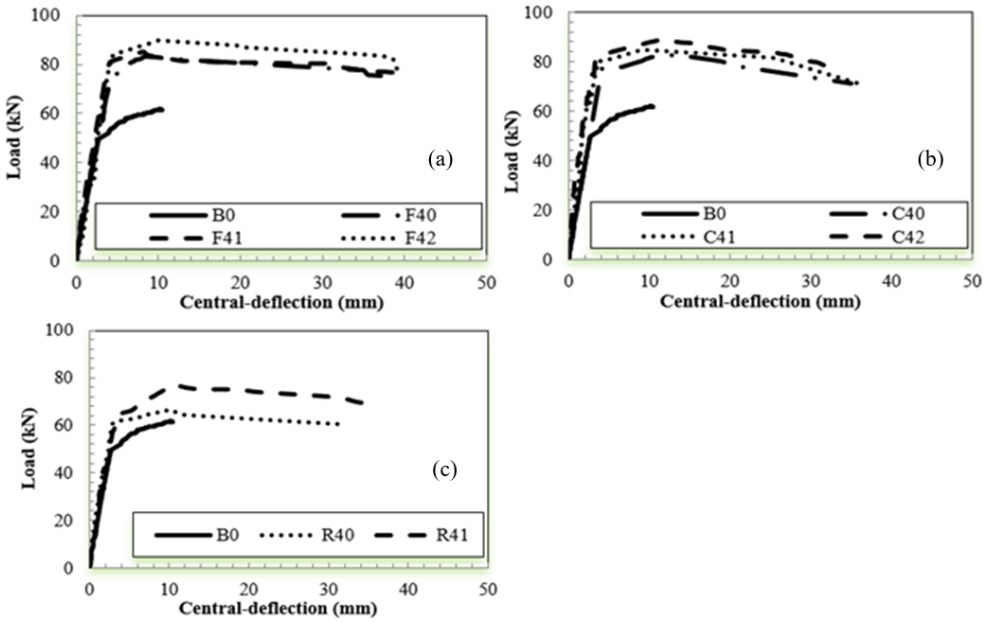

Figure 7. All load–displacement curves: (a) Load–displacement curves for samples reinforced with flat steel plates; (b) Load–displacement curves for samples reinforced with curved steel plates; (c) Load–displacement curves for samples reinforced with rounded steel plates

Table 4. All experimental results

Beams	Cracking State		Yielding State		Ultimate State		P_u Increase (%)	Δ_{max} (mm)	Ductility Index (%)	Ductility Index Increase (%)	Stiffness (kN/mm)	Stiffness Increase (%)
	P_{cr} (kN)	Δ_{cr} (mm)	P_y (kN)	Δ_y (mm)	P_u (kN)	Δ_u (mm)						
B0	9	0.51	51.54	3	61.89	10.18	0	10.37	3.46	0	17.08	0
F40	13	0.49	73.14	3.75	83.5	8.48	34.91	38	10.13	193.1	18.43	7.94
F41	13	0.47	81.11	3.85	85.17	8.12	37.61	39.8	10.34	199	20.12	17.85
F42	19	1.15	84.02	3.75	89.84	10	45.15	39.2	10.45	202.4	25	46.42
C40	12	0.8	72.2	4.1	82.72	14	33.65	35	8.54	146.9	18.24	6.81
C41	14	0.41	79.45	3.6	84.85	9.1	37.1	36.4	10.11	192.3	20.52	20.17
C42	19	0.24	80.63	3.4	88.76	10.4	43.41	33	9.71	180.8	19.49	14.11
R40	10	0.52	60.5	3.24	66.64	10.17	7.67	33	10.19	194.6	18.57	8.71
R41	23	1.16	64.9	3.4	77.11	10.51	24.59	35	10.29	197.8	18.71	9.52

Moreover, the constraining of steel plates has improved the yield and peak load, so constraining the flat plate with two inclined steel plates by 45° on both sides has enhanced the yield and peak load by 14.9% and 7.6%, respectively, as compared with no constraining specimen which results from the increase of bond strength between the plate and concrete. Otherwise, the use of curved steel plate has improved the yield and ultimate capacity with ratios lower than those ratios in case of using flat steel plate by differing of 1.82% and 1.26%, respectively, due to approaching the peak of the curve to the neutral axis. Finally, the effect of the rounded steel plate was lower than the two above configurations since the amount of steel plate in the tension zone of RC was lower than other configurations. Also, the constraining of the curved and rounded steel plates enhanced the yield and ultimate loads by 11.68%, 7.3%, 7.27% and 15.71%, respectively, compared to no constrained steel plates due to the same reasons stated earlier.

3.3 Ductility Index

It is credible to define ductility as the capability of member/material to afford deformations beyond the limit of elastic whereas affording sensible load-carrying capacity pending total failure [26]. For RC beams, ductility can

be determined depending on the amount of tension and compression reinforcement, ductility and strength of the materials [27–29].

Eq. (1) can be used to calculate ductility.

$$\text{Ductility index} = \frac{\delta_{\max}}{\delta_y} \tag{1}$$

where, $\delta_{\max}$ and δ_y were the maximum and yield deflection, respectively.

According to Foster and Attard [30], the yielded deflection can be determined from the load–deflection curve in three steps, as illustrated in Figure 8.

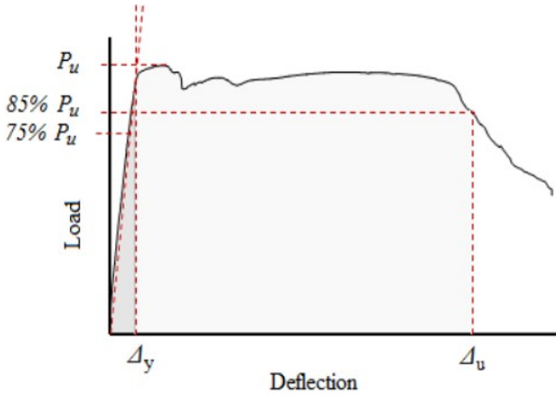

Figure 8. Calculation of ductility

Table 4 and Figure 9 present the ductility index at failure load compared with the reference beam. The ductility improved with the use of steel plates because of the flexure failure mode (i.e., the crush of concrete happens gradually before the rebar yield). Further, the average increase in ductility as compared with the reference beam was 188.4%. Regarding specimens reinforced with flat steel plate, it is noticed that the ductility was increased up to 193.1% compared to the reference beam. With the constraining of steel plates, the ductility was increased when constraining the flat steel plate with two inclined steel plates by 45° on both sides up to 3.16% compared to no constrained steel plates, the reason behind that is the improvement of interface bonding between the plate and the concrete. For the same reasons discussed in section 3.2, reinforcing with curved and rounded steel plates enhanced the ductility with lower ratios than the flat one, with differences of 28.9% and 48.2%, respectively. A noticeable enhancement of the ductility by 18.43% was achieved when curved steel plates constrained from both sides by vertical steel plates which results from the bond development between steel plates and concrete, further the increase in deflection prior the peak load. Finally, the constraining of rounded steel plate enhances the ductility index by 0.98% compared to no constrained one.

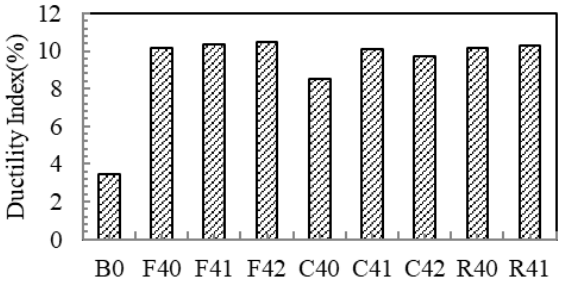

Figure 9. Ductility index for all specimens

3.4 Stiffness

The stiffness is defined as the capability of the member to prevent deflection or to bend under loading. Stiffness depends on the properties and geometry of materials and is considered one of the most significant characteristics of the RC members under serviceability behaviour. There are many parameters affected by Stiffness, such as deflection, ductility, and crack patterns. Stiffness can be calculated as a gradient of the load-displacement curve at the service

load state. From Figure 10 and Table 4, a noticeable increase in stiffness was perceived by using steel plates by an average of 16.44% as compared with the reference beam. On average, the use of a flat steel plate improved stiffness by an average increase of 11.9% compared to the reference beam, and it was higher than the specimens that were reinforced with a curved and rounded steel plates by an average difference 1.97% and 3.72%, respectively. The constraining of flat steel plates with two inclined steel plates has improved the stiffness by 35.65% compared with no constrained steel-plated specimen and due to more bond between steel plate and concrete resulting from constraining effect and delay of pre cracking appearance. Furthermore, the constraining effect on the curved and rounded plates were inferior to the flat one; stiffness in the specimen that reinforced with constrained curved steel plate showed an increase in stiffness by 12.5% than the no corresponding constrains one due to the same reasons stated above. Constraining the rounded steel plate from the center enhances stiffness by 0.73% compared to no constraint rounded steel-plated beam.

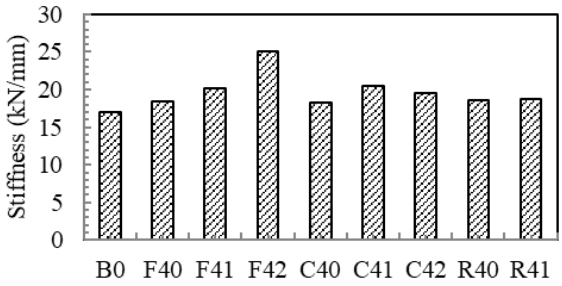

Figure 10. Stiffness values for all specimens

4 Numerical Study

4.1 Finite Element (FE) Models (Material Properties)

4.1.1 Steel bars

There are two stages: elastic and plastic to describe the qualities of steel material as in concrete.

Table 5 shows the Modulus of elasticity and Poisson's ratio of concrete for elastic behavior. Typically, Figure 11 shows an engineering stress-strain curve, which used to demonstrate the tension test of steel [31].

Table 5. Characteristics of concrete at elastic stage

Modulus of Elasticity (MPa)	Poisson's Ratio
15900	0.18 (assumed)

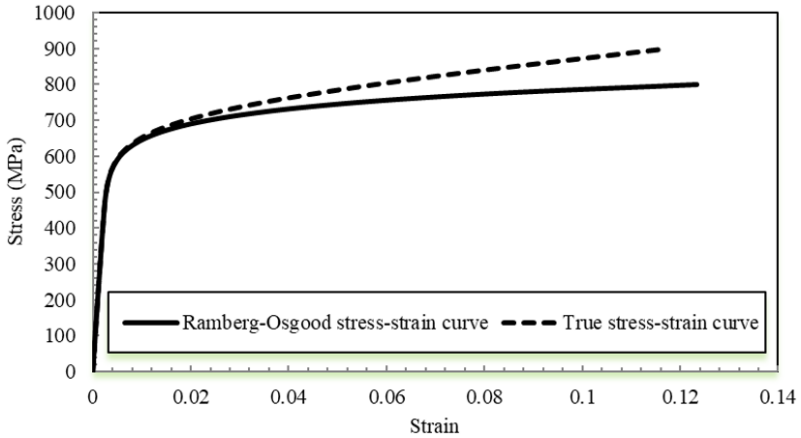

Figure 11. Stress-strain curve of steel bars

4.1.2 Concrete

Although it is well known that concrete exhibits brittle behavior, stress reflection may cause tensile cracks to close and for fractured pieces to converge. Therefore, damage models are the most effective technique to explain

how concrete behaves. There is a complexity of the behavior of the RC structures that is challenging to explain which results from the fact that concrete and steel behave differently. Because of all the aforementioned factors, the Concrete Damage Plasticity Model (CDP) was used to define the concrete [10, 11]. Most of the time, this model is excellent for presenting failure modes that depend on compression crushing and tensile cracking [32, 33]. The CDP model was conducted by Lubliner et al. [34] and developed by Lee and Fenves [35]. Consequently, represents the most often used model to simulate concrete in the ABAQUS software. Applications where materials were subjected to dynamic, monotonic, or cyclic loads are catered for by CDP models. Consequently, it enables recovery of stiffness during load reflections [36]. The concrete specimen's unloaded response is attenuated in Figure 12, because of the materials' degrading or being damaged by their elastic stiffness. Figure 11 damage variables, dt and dc, show how much strength has been lost or damaged. These variables have values ranging from 0 to 1, where 0 represents unharmed material and 1 represents complete loss of strength [36].

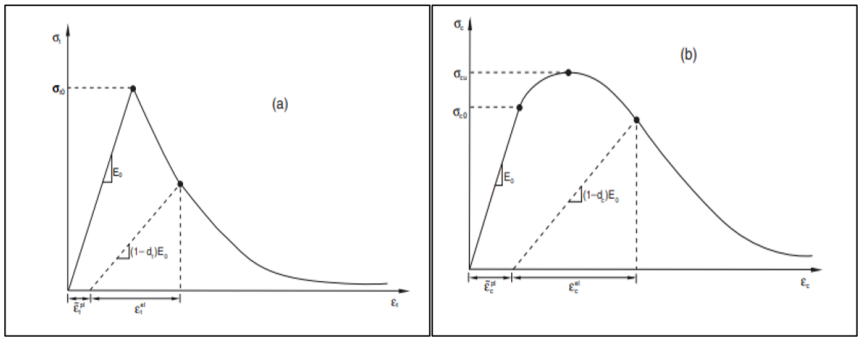

Figure 12. Uniaxial loading responses of concrete to: (a) Tension; (b) Compression [36]

Stress and inelastic strain measurements, along with the equations used in the definition of concrete from literature [14], were necessary to describe the compressive behavior. The inelastic, or crushing, strain was calculated based on Eq. (2).

$$\varepsilon_c^{\sim in} = \varepsilon_c - \varepsilon_{0c}^{el} \tag{2}$$

where,

$$\varepsilon_{0c}^{el} = \sigma_c / E_0 \tag{3}$$

$\boldsymbol{\varepsilon_c^{\sim in}}$: Inelastic strain;
$\boldsymbol{\varepsilon_c}$: Total strain;
$\boldsymbol{\varepsilon_{0c}^{ec}}$: Plastic strain;
$\boldsymbol{\sigma_c}$: Concrete's stress;
$\boldsymbol{E_0}$: Elastic modulus of undamaged concrete;
$\boldsymbol{d_c}$: The compression damage's parameter, calculated according to Eq. (4).

$$d_c = 1 - \frac{\sigma_c}{\sigma_c \max} \tag{4}$$

For $\sigma_c \geq {\sigma_c}^{\max}$, $d_c = 0$ for $\sigma_c < {\sigma_c}^{\max}$.
Similarly, the damage parameter for tension behavior $\boldsymbol{d_t}$ can be calculated as in Eqs. (5)–(7).

$$\varepsilon_t^{\sim ck} = \varepsilon_t - \varepsilon_{0t}^{el} \tag{5}$$

$$\varepsilon_{0t}^{el} = \sigma_t / E_0 \tag{6}$$

$$d_t = 1 - \frac{\sigma_t}{{\sigma_t}^{\max}} \tag{7}$$

where, $\varepsilon_t^{\sim ck}$: Cracking strain.

Figure 13 demonstrates the compression and tension damage behavior parameters of concrete that were used in the CDP model. Overall, the adopted CDP parameters have been shown to provide reliable predictions of load–deflection behavior and crack development in concrete beams and were therefore deemed suitable for the present study.

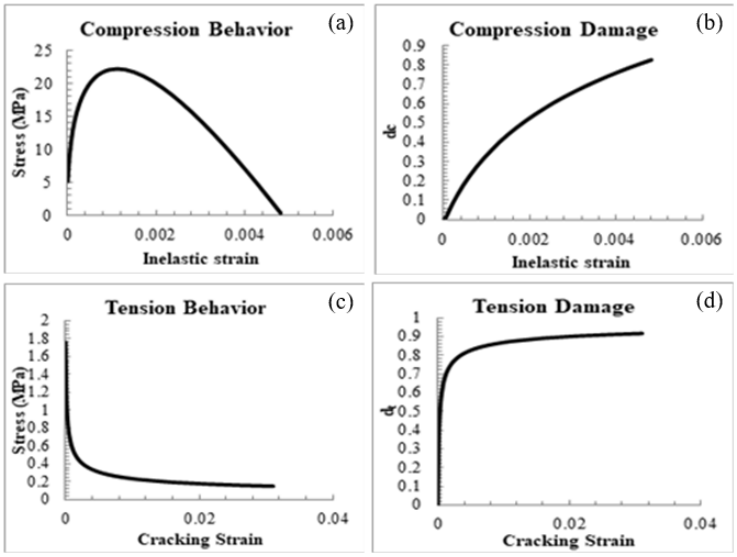

Figure 13. Characteristics of concrete in CDP model: (a) Compression behavior; (b) Compression damage; (c) Tension behavior; (d) Tension damage

Table 6 provides plastic parameters of concrete. Dilation angle, ψ is measured at high level and confining pressure in the p-q plane. The value is based on earlier research [37]. Eccentricity ε represents the small positive number that expresses the rate at which the asymptote of hyperbolic voltage approaches. Stress ratio, f_{b0}/f_{c0} is the proportion of the basic uniaxial and equi-biaxial compressive yield stresses. Ratio of the second stress invariant, K is the ratio of the second stress invariants on the meridian of tension to the second stress invariants on the meridian of compression at initial yield of any value of the pressure invariants. Viscosity parameter, μ is a component of CDP material behavior; in Abaqus/Standard, the default value is zero, although this is incorrect for nonlinear analysis. Consequently, it depends on the value from earlier studies [38].

Table 6. Parameters of concrete in plastic stage

Dilatation Angle (Degree)	Eccentricity	f_{b0}/f_{c0}	K	Viscosity Parameter
37	0.1	1.16	0.667	0.0005

4.2 Mesh Discretization and Boundary Conditions

In FE analysis, there are often two categories of elements employed in simulating the components of specimens: The C3D8R element, a linear brick element of an 8-node with reduced combination and hourglass control, is used for solid parts such as beams, bearings, and steel plates. Meanwhile the T3D2 element, a 2-node linear 3-D truss, is used for all types of reinforcement. After defining all necessary material characteristics in the models, the parts were assembled to create an entire model. Each model comprises of a single assembly. The size of the chosen mesh significantly impacts the accuracy of the results in FE analysis. According to Finite Element Method (FEM) theory, simulated models with small mesh sizes yield more accurate results but need longer computation times; in contrast, when the size is bigger [39]. A convergence analysis was carried out to determine the optimal mesh size. It was observed that reducing the mesh size to 15 mm showed a tolerance of 2% in the predicted ultimate load. Therefore, a mesh size of 15 mm was selected as an optimal size for each region of the model (see Figure 14).

The original boundary conditions were indicated along the width of the steel support, particularly on the partition line, as indicated in Figure 15. The beams are simply supported, so two steel plates were modeled in the part module and the properties of steel were provided accordingly.

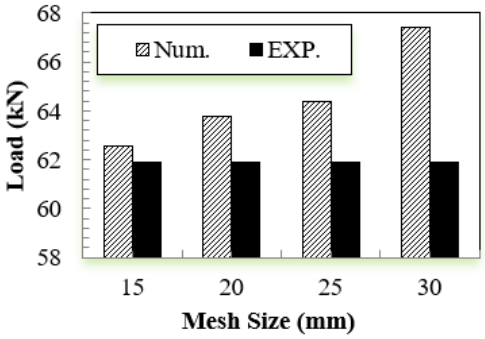

Figure 14. Mesh size convergence study

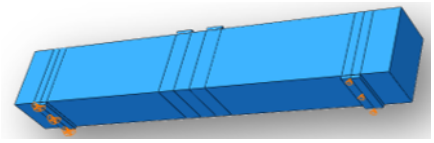

Figure 15. Boundary condition

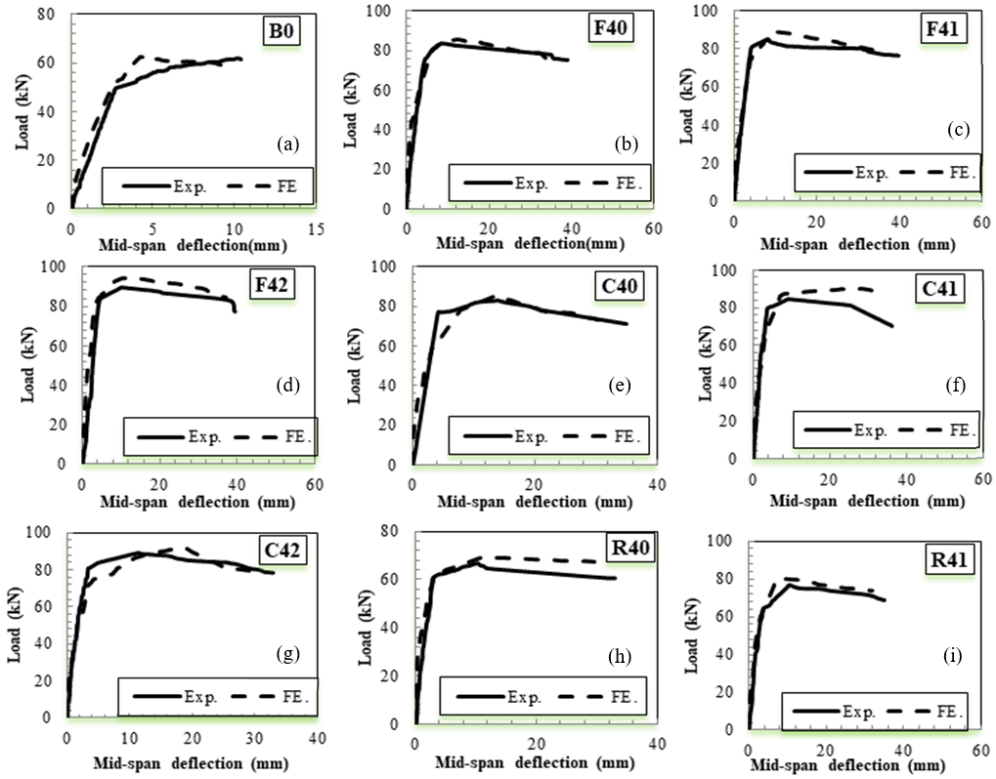

Figure 16. Load–displacement curves for all tested beams: (a) Load–displacement curves for B0 beam; (b) Load–displacement curves for F40 beam; (c) Load–displacement curves for F41 beam; (d) Load–displacement curves for F42 beam; (e) Load–displacement curves for C40 beam; (f) Load–displacement curves for C41 beam; (g) Load–displacement curves for C42 beam; (h) Load–displacement curves for R40 beam; (i) Load–displacement curves for R41 beam

4.3 FE Modelling (Results and Discussion)

4.3.1 Model verification

Figure 16 displays a comparison between experimental and FE load-displacement curves for all specimens. This illustration demonstrates that most FE curves show higher stiffness after initial cracking compared to their equivalent experimental curves. To distribute an infinitely free structure to one with limited freedom. The FE curves growth

with higher slope than the experimental curves because of this fact, which causes an increase in load and a decrease in deflection. This is attributed to idealized material assumptions, perfect bond conditions, and the absence of micro-cracking and construction imperfections in the numerical model, which are inherently present in experimental specimens.

The most significant element in this experimental design is the spread of hairline fractures in the concrete. Since hairline cracks are not accounted for in FE models, the handling of specimens may produce additional hairline fractures, that reduce the stiffness of experimental beams. However, the general trend of the load-displacement of experimental and FE curves demonstrates a good agreement. Despite counting all of Bäker's suggestions [40], a margin of discrepancy between the experimental and FE results remains, with the ultimate load difference varying up to 6.13%. As indicated in Table 7, the load ratios between experimental and FE ultimate loads ranged between 0.94 and 0.99%, and the deflection ratios between experimental and FE ultimate loads ranged between 0.69 and 2.38%.

Table 7. Experimental and FEM results comparison

Beam	P_u Exp. (kN)	P_u FE (kN)	P_u Exp./FE	δ_u Exp. (mm)	δ_u FE (mm)	δ_u Exp./FE
B0	61.89	62.54	0.99	10.18	4.27	2.38
F40	83.5	86.3	0.97	8.45	12.21	0.69
F41	85.17	89.56	0.95	8.12	9.11	0.89
F42	89.84	94.44	0.95	10	10.57	0.94
C40	82.72	84.09	0.98	14	13.82	1.01
C41	84.85	90.39	0.94	9.1	8.12	1.12
C42	88.76	91.99	0.96	10.4	13.9	0.75
R40	66.64	69.51	0.96	10.17	11	0.92
R41	77.11	80.67	0.96	10.51	7.31	1.44

4.3.2 Crack propagation and failure mechanisms

This section examines the crack growth to verify the model's accuracy against the outcomes of the experimental work. The formation of cracks might be accurately predicted using the ABAQUS algorithm. The tension mid-span zone was where the cracks first developed, which is consistent with the numerical findings. For most experimental and FE specimens, Figure 17, Figure 18, Figure 19, and Figure 20 depict the crack patterns caused by flexural and compression damage. Under flexural mode, every beam broke. Additionally, the severe tension fiber of the beams in the areas subjected to the greatest bending moment is where the tensile damage first manifested itself. The term "compression damage" refers to the crush that develops prior to reinforcement yielding and foretells beam failure.

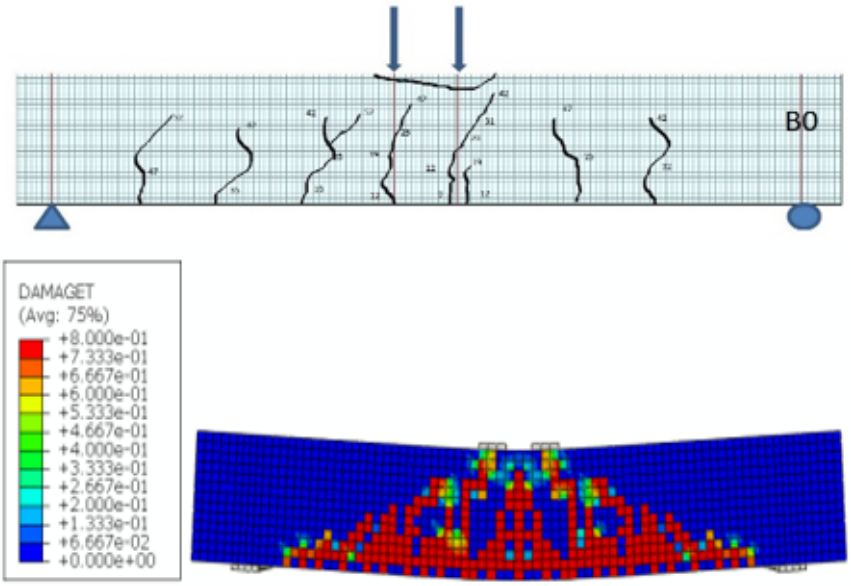

Figure 17. Crack patterns for experimental and FE B0 beam

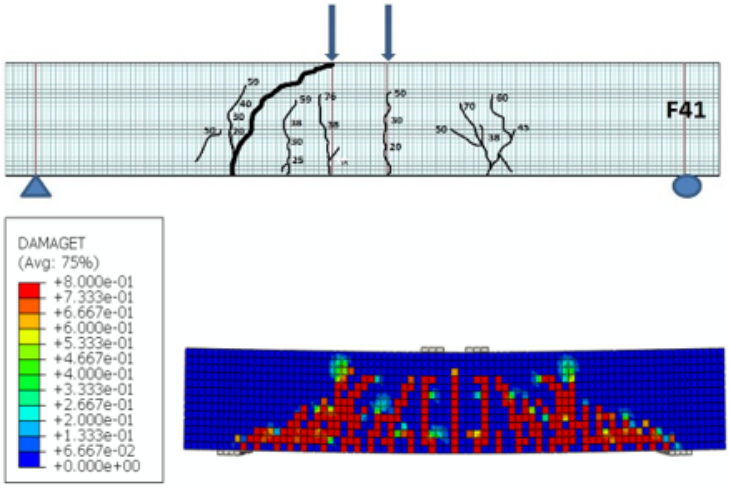

Figure 18. Crack patterns for experimental and FE F41 beam

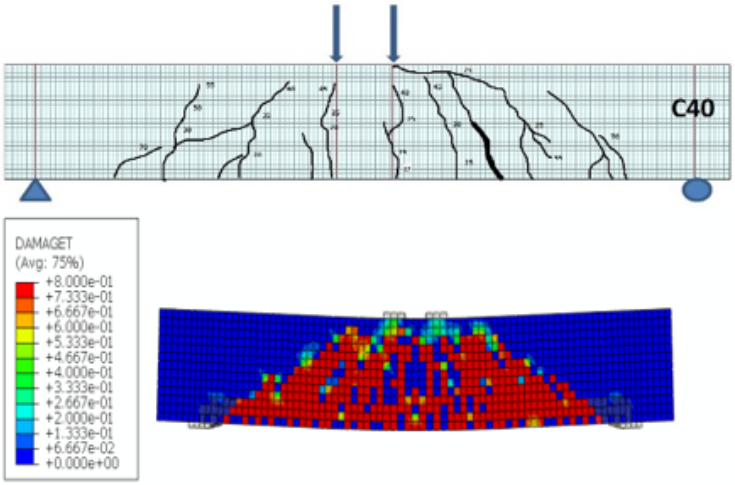

Figure 19. Crack patterns for experimental and FE C40 beam

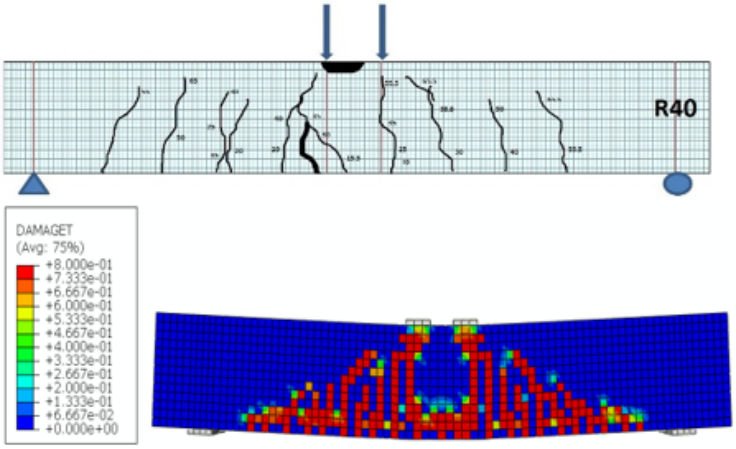

Figure 20. Crack patterns for experimental and FE R40 beam

5 Conclusions

The experimental investigation assessed the ductility and flexural behavior of steel-plate-RC beams. The results from experimental data and the numerical analysis can be summarized follow:

• Flexural reinforcing of concrete beams by using steel plates was effective and significantly enhanced the

flexural performance due to delaying the first cracking appearance and increasing the ultimate load up to 45.15% in comparison with the reference beam.

• An improvement up to 35% of the ultimate load was observed for beams with flat steel plates compared with the reference beam.

• Adding two inclined steel plates by 45° on both sides to the flat steel plates improved their yield and ultimate load by 21.1% and 10%, respectively.

• The load-deflection curve characteristics were enhanced, and the beams behaved more flexure post-peak load until failure.

• Specimens containing steel plates display more ductile behavior than the reference beam, specifically beam F42 which showed 202.4% increase of the ductility as compared with the reference beam. Also, the constraint of the steel plates can improve the ductility behavior by an increase up to 3.16% compared to no constraining specimen.

• The stiffness can be enhanced by employing steel plates with an increase of 46.42% compared to the reference beam. The stiffness was further increased when constraining flat, curved, and rounded steel plates up to 35.65%, 12.5%, and 0.73%, respectively, compared to their corresponding no constraining specimens.

• There was good agreement in the results between experimental and FE works, with 6.13% as the highest difference in ultimate load. However, the elastic behavior of the modeled beams was stiffer compared with their experimental counterparts.

Data Availability

The data used to support the findings of this study are available from the corresponding author upon request.

Conflicts of Interest

The authors declare that they have no conflicts of interest.

References

[1] D. Zhang, T. Ueda, and H. Furuuchi, "Concrete cover separation failure of overlay-strengthened reinforced concrete beams," *Constr. Build. Mater.*, vol. 26, no. 1, pp. 735–745, 2012. https://doi.org/10.1016/j.conbuildmat.2011.06.082

[2] S. Kothandaraman and G. Vasudevan, "Flexural retrofitting of RC beams using external bars at soffit level: An experimental study," *Constr. Build. Mater.*, vol. 24, no. 11, pp. 2208–2216, 2010. https://doi.org/10.1016/j.conbuildmat.2010.04.036

[3] C. E. Chalioris, G. E. Thermou, and S. J. Pantazopoulou, "Behaviour of rehabilitated RC beams with self-compacting concrete jacketing: Analytical model and test results," *Constr. Build. Mater.*, vol. 55, pp. 257–273, 2014. https://doi.org/10.1016/j.conbuildmat.2014.01.031

[4] S. Yang, S. Cao, and R. Gu, "New technique for strengthening reinforced concrete beams with composite bonding steel plates," *Steel Compos. Struct.*, vol. 19, no. 3, pp. 735–757, 2015. https://doi.org/10.12989/scs.2015.19.3.735

[5] A. Demir, E. Ercan, and D. D. Demir, "Strengthening of reinforced concrete beams using external steel members," *Steel Compos. Struct.*, vol. 27, no. 4, pp. 453–464, 2018. https://doi.org/10.12989/scs.2018.27.4.453

[6] Y. F. Wu and K. Liu, "Characterization of mechanically enhanced FRP bonding system," *J. Compos. Constr.*, vol. 17, no. 1, pp. 34–49, 2013. https://doi.org/10.1061/(ASCE)CC.1943-5614.0000302

[7] B. H. Osman, E. Wu, J. Bohai, and M. Abdallah, "Repair technique of pre-cracked reinforced concrete beams with transverse openings strengthened with steel plate under sustained load," *J. Adhes. Sci. Technol.*, vol. 31, no. 21, pp. 2360–2379, 2017. https://doi.org/10.1080/01694243.2017.1301073

[8] S. Qin, S. Dirar, J. Yang, A. H. C. Chan, and M. Elshafie, "CFRP shear strengthening of reinforced-concrete T-beams with corroded shear links," *J. Compos. Constr.*, vol. 19, no. 5, p. 04014081, 2015. https://doi.org/10.1061/(ASCE)CC.1943-5614.0000548

[9] E. M. Lotfy, "Flexural strengthening of RC beams," *Int. J. Eng. Technol. Res.*, vol. 6, no. 3, pp. 83–86, 2016.

[10] R. K. L. Su, W. Y. Lam, and H. J. Pam, "Behaviour of embedded steel plate in composite coupling beams," *J. Constr. Steel Res.*, vol. 64, no. 10, pp. 1112–1128, 2008. https://doi.org/10.1016/j.jcsr.2007.09.013

[11] N. K. Subedi and N. R. Coyle, "Improving the strength of fully composite steel–concrete–steel beam elements by increased surface roughness: An experimental study," *Eng. Struct.*, vol. 24, no. 10, pp. 1349–1355, 2002. https://doi.org/10.1016/S0141-0296(02)00070-6

[12] R. K. L. Su, W. Y. Lam, and H. J. Pam, "Experimental study of plate-reinforced composite deep coupling beams," *Struct. Des. Tall Spec. Build.*, vol. 18, no. 3, pp. 235–257, 2009. https://doi.org/10.1002/tal.407

[13] H. Metawei, D. Arafa, and N. A. Taha, "Flexural performance of beams reinforced by checker steel using roughness methods," in *Proceedings of the International Conference on Advances in Steel Structures Egypt Steel 2019 (ES19)*, 2019, pp. 17–19.

[14] M. M. Sarhan, M. N. S. Hadi, and L. H. Teh, "Strength and ductility behaviour of steel plate reinforced concrete beams under flexural loading," in *Proceedings of the 1st International Conference on Structural Engineering Research (iCSER2017), Sydney, Australia*, 2017, pp. 161–166.

[15] A. M. Ibrahim, Z. S. Khaled, and I. M. A. Ameer, "Effect of using internal steel plates for shear reinforcement on flexural behavior of self-compacting concrete beams," *Al-Nahrain J. Eng. Sci.*, vol. 20, no. 5, pp. 1071–1082, 2017.

[16] H. K. Ammash, "Behavior of reinforced concrete beams using steel strips as shear reinforcements," *Int. J. Appl. Eng. Res.*, vol. 12, no. 19, pp. 8681–8688, 2017.

[17] A. M. Ibrahim, M. J. Hamood, and A. A. Mansor, "Behaviour of wide reinforced concrete beams with different shear steel plates spacing," *J. Eng. Sustain. Dev.*, vol. 20, no. 5, pp. 120–135, 2016.

[18] D. Liu, Z. Jiang, X. Long, K. Duan, and M. Li, "Comparison of flexural performance of reinforced concrete beams reinforced with steel plates and corrugated steel plates," *Case Stud. Constr. Mater.*, vol. 21, p. e04047, 2024. https://doi.org/10.1016/j.cscm.2024.e04047

[19] W. Q. Ding, Y. J. Guo, S. B. Li, X. R. Li, and Q. Z. Zhang, "Experimental research on the mechanical behavior of segmental joints of shield tunnel reinforced with a new stainless steel corrugated plate," *Case Stud. Constr. Mater.*, vol. 18, p. e02170, 2023. https://doi.org/10.1016/j.cscm.2023.e02170

[20] S. Y. Yu, G. K. Zhang, Z. Wang, J. Liu, S. X. Deng, X. Z. Song, and M. Y. Wang, "Experimental and numerical study of corrugated steel–plain concrete composite structures under contact explosions," *Thin-Walled Struct.*, vol. 197, p. 111624, 2024. https://doi.org/10.1016/j.tws.2024.111624

[21] B. L. Zhu, W. H. Bai, C. B. Wen, J. Q. Zuo, H. J. Sun, X. Wang, and Y. L. Guo, "Experimental and numerical investigation into hysteretic performance of orthogonal double corrugated steel plate shear walls," *Thin-Walled Struct.*, vol. 195, p. 111392, 2024. https://doi.org/10.1016/j.tws.2023.111392

[22] X. Feng, D. Liu, X. Long, K. Duan, J. Zuo, W. Liu, and H. Dong, "Flexural capacity of the normal sections of concrete beams strengthened with corrugated steel plates," *Buildings*, vol. 14, no. 5, p. 1398, 2024. https://doi.org/10.3390/buildings14051398

[23] ACI Committee, "Standard Practice for Selecting Proportions for Normal, Heavyweight, and Mass Concrete (ACI 211.1-91)," 1991. https://www.academia.edu/38504100/ACI_211_1_91_Standard_Practice_for_Selecting_Proportions_for_Normal_Heavyweight_and_Mass_Concrete

[24] ASTM International, "Standard Specification for Deformed and Plain Carbon-Steel Bars for Concrete Reinforcement," 2022. https://store.astm.org/a0615_a0615m-20.html

[25] ASTM International, "Standard Test Methods and Definitions for Mechanical Testing of Steel Products," 2017. https://store.astm.org/a0370-05.html

[26] R. Park, "Ductility evaluation from laboratory and analytical testing," in *Proceedings of the 9th World Conference on Earthquake Engineering*, Tokyo–Kyoto, Japan, 1988, pp. 605–616.

[27] K. E. Leslie, K. S. Rajagopalan, and N. J. Everard, "Flexural behavior of high-strength concrete beams," *ACI J. Proc.*, vol. 73, no. 9, pp. 517–521, 1976. https://doi.org/10.14359/11093

[28] S. W. Shin, S. K. Ghosh, and J. Moreno, "Flexural ductility of ultra-high-strength concrete members," *ACI Struct. J.*, vol. 86, no. 4, pp. 394–400, 1989. https://doi.org/10.14359/2877

[29] S. Sarkar, O. Adwan, and J. G. L. Munday, "High strength concrete: An investigation of the flexural behaviour of high strength RC beams," *Struct. Eng.*, vol. 75, no. 8, pp. 115–121, 1997.

[30] S. J. Foster and M. M. Attard, "Experimental tests on eccentrically loaded high-strength concrete columns," *ACI Struct. J.*, vol. 94, no. 3, pp. 295–303, 1997. https://doi.org/10.14359/481

[31] P. S. Patwardhan, R. A. Nalavde, and D. Kujawski, "An estimation of Ramberg–Osgood constants for materials with and without lüders strain using yield and ultimate strengths," *Procedia Struct. Integr.*, vol. 17, pp. 750–757, 2019. https://doi.org/10.1016/j.prostr.2019.08.100

[32] B. Alfarah, F. López-Almansa, and S. Oller, "New methodology for calculating damage variables evolution in plastic damage model for RC structures," *Eng. Struct.*, vol. 132, pp. 70–86, 2017. https://doi.org/10.1016/j.engstruct.2016.11.022

[33] C. B. L. Ruska and M. W. Bøgh, "Finite element modelling of reinforced concrete elements," mastersthesis, Aalborg University, 2019.

[34] J. Lubliner, J. Oliver, S. Oller, and E. Oñate, "A plastic-damage model for concrete," *Int. J. Solids Struct.*, vol. 25, no. 3, pp. 299–326, 1989. https://doi.org/10.1016/0020-7683(89)90050-4

[35] J. Lee and G. L. Fenves, "Plastic-damage model for cyclic loading of concrete structures," *J. Eng. Mech.*, vol.

124, no. 8, pp. 892–900, 1998. https://doi.org/10.1061/(ASCE)0733-9399(1998)124:8(892)

[36] Dassault Systemes, "Abaqus Theory Manual," 2016. http://orpheus.nchc.org.tw:2080/v6.12/books/stm/default.htm?startat=ch03s05ath73.html

[37] Y. Sümer and M. Aktaş, "Defining parameters for concrete damage plasticity model," *Challenge J. Struct. Mech.*, vol. 1, no. 3, pp. 149–155, 2015. https://doi.org/10.20528/cjsmec.2015.07.023

[38] A. Demir, H. Ozturk, K. Edip, M. Stojmanovska, A. Bogdanovic, and E. Seismology, "Effect of viscosity parameter on the numerical simulation of reinforced concrete deep beam behavior," *Online J. Sci. Technol.*, vol. 8, no. 3, pp. 50–56, 2018.

[39] S. T. More and R. S. Bindu, "Effect of mesh size on finite element analysis of plate structure," *Int. J. Eng. Sci. Innov. Technol.*, vol. 4, no. 3, pp. 181–185, 2015.

[40] M. Bäker, "How to get meaningful and correct results from your finite element model," *arXiv preprint arXiv:1811.05753*, 2018. https://doi.org/10.48550/arXiv.1811.05753